Indian Journal of Experimental Biology
Vol. 45, January 2007, pp. 48-57

Localization of protein-protein interactions in live cells using confocal and spectral imaging FRET microscopy

Ye Chen & Ammasi Periasamy*

Departments of Biology and Biomedical Engineering, W M Keck Center for Cellular Imaging, Gilmer Hall, University of Virginia, Charlottesville, VA 22904, USA

Received 10 May 2006

Microscopy has become an essential tool for cellular protein investigations. The development of new fluorescent markers such as green fluorescent proteins generated substantial opportunities to monitor protein-protein interactions qualitatively and quantitatively using advanced fluorescence microscope techniques including wide-field, confocal, multiphoton, spectral imaging, lifetime, and correlation spectroscopy. The specific aims of the investigation of protein dynamics in live specimens dictate the selection of the microscope methodology. In this article confocal and spectral imaging methods to monitor the dimerization of alpha enhancer binding protein (C/EBPα) in the pituitary GHFT1-5 living cell nucleus have been described. Also outline are issues involved in protein imaging using light microscopy techniques and the advantages of lifetime imaging of protein-protein interactions.

Keywords: C/EBPα, Confocal, Fluorescent proteins, FRET, Microscopy, Protein-protein interactions, Protein localization, Spectral Imaging,

Microscopes have been an essential tool found in virtually every biological laboratory following the observation and description of protozoa, bacteria, spermatozoa, and red blood cells by Antoni van Leeuwenhoek, in the 1670's[1,2]. The ability to study the development, organization, and function of unicellular and higher organisms and to investigate structures and mechanisms at the microscopic level has allowed scientists to better grasp the often misunderstood relationship between microscopic and macroscopic behavior. Further, the microscope preserves temporal and spatial relationships that are frequently lost in traditional biochemical techniques and gives two- or three-dimensional resolutions that other laboratory methods cannot. The benefits of fluorescence microscopy techniques are numerous[3-7]. The inherent specificity and sensitivity of fluorescence, the high temporal, spatial, and three-dimensional resolution that is possible, and the enhancement of contrast resulting from detection of an absolute rather than relative signal (i.e. unlabeled features usually do not emit, although some techniques utilize natural autofluorescence) are several advantages of fluorescence techniques. Additionally, the plethora of well-described spectroscopic techniques providing different types of information, and the commercial availability of fluorescent probes, many of which exhibit an environment- or analytic-sensitive response, broaden the range of possible applications. Recent advancements in light sources, detection systems, data acquisition methods, image enhancement, analysis and display methods have further broadened the applications in which fluorescence microscopy can successfully be applied[3-5]. In particular, fluorescent probes can be used to target many cellular components to follow cell signaling in space (nanometer to meter) and time (nanoseconds to days)[8].

Förster (or fluorescence) resonance energy transfer (FRET) methodology has been implemented in these sensitive fluorescence microscopy techniques to monitor protein-protein interactions in living or fixed specimens[4]. Wide-field FRET (W-FRET) imaging provides the 2-D spatial distribution of steady-state protein-protein interactions[3-4,9,10]. In addition, the W-FRET system allows the use of any excitation wavelength using interference filters for various

*Correspondent author
Phone: 434-243-7602 or 982-4869
Fax: 434-982-5210
Email: ap3t@virginia.edu

fluorophore pairs. The disadvantage of W-FRET is that it contains out-of-focus information in the FRET signal[9]. However, this low cost system is used widely to monitor protein associations in living specimen where confocality is not an issue, such as following events in the nucleus. In confocal FRET (C-FRET) and two-photon (2p) excitation FRET (2p-FRET) microscopy one can discriminate the out-of-focus information to obtain the FRET signal at the selected focal plane[4,11-13]. Moreover, 2p-FRET microscopy uses infrared (IR) laser light as an excitation wavelength and has the ability to excite most of the selected fluorophore pairs compared to the confocal systems where fixed laser lines are available at few limited excitation wavelengths[12]. It is important to choose 2p-FRET fluorophore pairs with different 2p absorption cross section to avoid simultaneous excitation by one wavelength. As an example, the conventional one-photon FRET pair fluorescein and rhodamine may not be a good 2p-FRET fluorophore pair since both are excitable around 790 nm. But fluorescein (or Alexa488) and Cy3 (or Alexa555) are an ideal pair for 2p-FRET imaging[11]. The use of infrared laser light excitation instead of ultra-violet laser light also reduces phototoxicity in the living cell. In general, the 2p-FRET microscopy is superior for deep tissue FRET imaging[11] rather than monolayer cells, particularly cells that express mutant forms of green fluorescent proteins as they potentially are excited by one wavelength[12].

Spectral imaging, either by confocal or two-photon systems, is an intensity-based imaging technique which provides an excellent way to obtain a FRET signal. All these techniques require the removal of certain signal contaminations, discussed later. Fluorescence lifetime microscopy (FLIM) avoids some of these difficulties, but is technically challenging. Measuring the donor quenching or donor lifetime provides a method for estimating energy transfer efficiency (E%)[12-19].

In this paper the data acquisition and processing methodology involved in FRET imaging, using confocal microscopy techniques to localize the C/EBPα dimerization in live cell nucleus have been described. The usage of spectral imaging techniques for FRET and the advantages and simplicity in interpreting the protein dimerization using fluorescence lifetime imaging (FLIM) combined with FRET techniques have also been described.

Materials and Methods

What is FRET?

Förster (or fluorescence) resonance energy transfer (FRET) is a process involving the radiationless transfer of energy from a donor fluorophore to an appropriately positioned acceptor fluorophore[20-22]. (i) FRET can occur when the emission spectrum of a donor fluorophore significantly overlaps (>30%) the absorption spectrum of an acceptor (Fig. 1). If the spectrum is not overlapped there cannot be any FRET. (ii) The emission dipole of the donor and the acceptor absorption dipole must be oriented to each other and it must not be oriented perpendicular to each other. Dipole is an electromagnetic field that exists in a molecule that has one region with oppositely charged areas, a negative charge and another region with a positive charge. If the spectra are overlapped, the

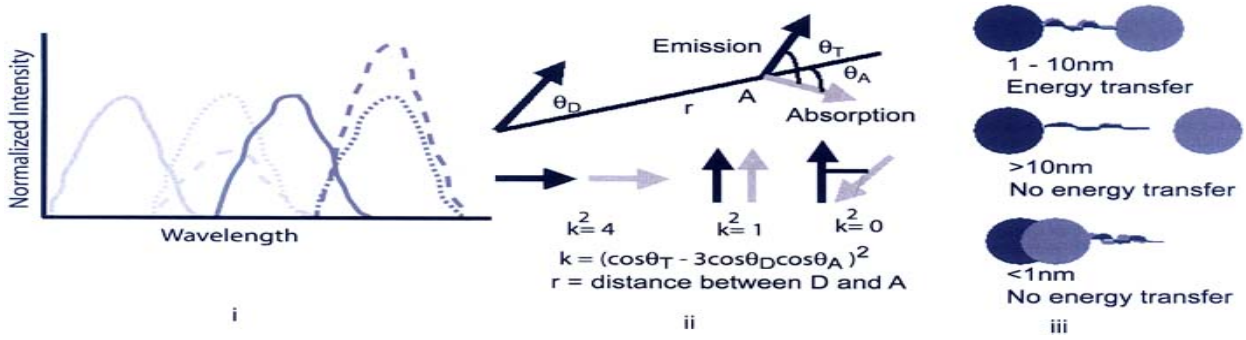

Fig. 1 — Illustration of three conditions for FRET to occur. (i) Spectral overlap. Donor (D) emission of one of the fluorophore (smaller broken line) should overlap (>30%) to the acceptor (A) absorption (solid line) of another fluorophore. (ii) Dipole-dipole coupling. The donor emission dipole should orient with the acceptor absorption dipole in the range of 1-4 and (iii) Distance between donor and acceptor molecule should be within 1-10 nm. The larger broken line represents reduction in emission of D and increase in emission of A (sensitized emission). Solid lines-absorption spectra; smaller broken lines-emission spectra.

donor's oscillating emission dipole will look for a matching absorption dipole of an acceptor to oscillate in synchrony. The magnitude of the relative orientation of the dipole-dipole coupling values is 1-4. (iii) Because the efficiency of energy transfer varies inversely with the sixth power of the distance separating the donor and acceptor fluorophores, the distance over which FRET can occur is limited to between 1-10 nm[21]. When the spectral, dipole orientation, and distance criteria are satisfied, excitation of the donor fluorophore results in sensitized fluorescence emission of the acceptor, indicating that the tagged proteins are separated by < 10 nm. This FRET-based inferred proximity between two labeled cellular components considerably surpasses the resolution of general light-microscopy which at best can resolve distances of ~ 200 nm.

Protein-protein interactions mediate the majority of cellular processes. Identification of a protein's interacting partners is critical in understanding its function, placing it in a biochemical pathway, and thereby establishing its relationship to important disease processes. Protein localization studies using microscopy techniques can indicate what proteins are expressed, where proteins are expressed, and where they go over time. Tracking these parameters would allows us to gain a greater understanding of these proteins' functions and determine for example, which are likely to be the best drug targets. The monitoring of protein associations in living specimens and the accuracy of FRET measurement using microscopic techniques has tremendously increased since 1997 after the introduction of various mutant forms of Green fluorescent proteins (GFPs)[4,13,23-28].

Instrumentation

Here we describe a confocal/multiphoton/spectral imaging Zeiss 510 microscope system. The system consists of a Zeiss Axiovert 200M epifluorescent microscope with a 100W Hg Arc Lamp with a halogen lamp and a transmission detector. This is a motorized microscope and the LSM software automatically identifies the microscope settings and the objective used, and controls the focus movements of the microscope parts with high precision. A Plan-Apochromat 63x oil NA 1.4 objective lens was used for imaging the protein molecules. This Axiovert 200M is coupled to a Zeiss510 confocal/multiphoton/ spectral imaging system (www.zeiss.de). A 10W Verdi pumped, tunable (model 900 Mira, www.coherentinc.com) modelocked ultrafast (78 MHz) pulsed (<150 femtosecond; tunable 700-1000 nm) laser is directly coupled to the laser port of Zeiss510. For confocal imaging, the system consists of a 45mW argon laser (457, 488, 514 nm), a 10mW He-Ne laser (561 nm) and a diode 633 nm laser. These lasers were combined and fiber-optically coupled to the laser port of the Zeiss510 scanning head. By means of an AOTF (acousto-optical tunable filter; for confocal) or AOM (acousto-optical modulator; for multiphoton), the excitation light can be exactly intensity-controlled and blanked or unblanked precisely down to one pixel. This provides the best possible specimen preservation and enables targeted photobleaching. The system is equipped with three internal detectors (photomultiplier tube, PMT, for fluorescence imaging) equipped with respective emission filter wheels. It contains motor-driven collimators, scanning mirrors, individually adjustable and positionable pinholes and highly sensitive PMT detectors. The system software enables sophisticated functions such as multitracking, spot scan, fast step scan, time-lapse or series, ROI (region of interest) scan and ROI bleaching. Appropriate emission filter were used to collect the quenched donor and sensitized FRET signal from the FRET pairs CFP-YFP (Cyan- and Yellow fluorescent protein)[4,28] and Cerulean-Venus[23].

The system is also equipped with a highly sensitive 32 channels spectral detector. This very efficient optical grating provides an innovative way of separating fluorescence emissions in the META detector. Thus, the spectral signature is acquired for each pixel (confocal or multiphoton) of the scanned image and subsequently can be used for the digital separation of the component dyes. No emission filter is involved in this configuration. A mathematical algorithm is implemented on the collected spectral image cube or lambda stack of the collected images at selected wavelength bands[29,30]. A lambda stack is a series of x-y images that sample emission wavelengths from a range of small wavelength bands (10 nm). Lambda stacks can be considered in much the same way as a time series or z-dimension series. The x-y images can be viewed along the wavelength axis to determine how the intensity of pixels in the image changes at different emission bands and the emission spectra of a particular dye can be revealed by plotting the pixel intensity versus the center

wavelength of each emission band. The quality of the spectra obtained depends largely on the number of images collected at distinct wavelength bands, the size of the wavelength bands, and the sensitivity and reproducibility of the device used to collect the spectral images. A linear unmixing algorithm was performed in the lambda stack images to separate the respective spectra of individual dye by using the respective reference spectra of the dye used for lambda stack images[29,30].

Cell preparation

CAATT/enhancer binding protein alpha (C/EBPα): For the studies described here, the sequence encoding the DNA binding and dimerization domain of the transcription factor C/EBPα[31] was fused in-frame to commercially available CFP or YFP color variants (www.clontech.com) to generate CFP-C/EBPα and YFP-C/EBPα[32]. Mouse pituitary GHFT1-5 cells were harvested and transfected with the indicated plasmid DNA(s) by electroporation[33]. The total input DNA was kept constant using empty vector DNA. Cell extracts from transfected cells were analyzed by Western blot to verify the tagged proteins were of the appropriate size as described previously. For imaging, the cells were inoculated dropwise onto a sterile cover glass in 35 mm culture dishes and allowed to attach prior to gently flooding the culture dish with media. They were maintained for 18 to 36 hours prior to imaging. The cover glass with attached cells was inserted into a chamber containing the appropriate medium and the chamber was then placed on the microscope stage.

FRET data acquisition and analysis

One of the important conditions for FRET to occur is the overlap of the emission spectrum of the donor (D) with the absorption spectrum of the acceptor (A). Because of spectral overlap, the FRET signal is contaminated by donor emission into the acceptor channel and by the excitation of acceptor molecules by the donor excitation wavelength. The combination of these signals is called the spectral bleedthrough (SBT) signal into the acceptor (or FRET) channel[34]. In addition to SBT, other sources of noise contaminate the FRET signals, including spectral sensitivity variations in donor and acceptor channels, autofluorescence, and detector and optical noise[4,35,36].

In brief, to remove the SBT or cross-talk contained in the confocal FRET (C-FRET) signal, images were acquired as listed in Fig. 2. Cover slip contains cells expressed with CFP and YFP (D+A) were placed on the confocal/spectral imaging microscope stage in a specially designed chamber. These cells were excited with donor excitation wavelength 457 nm with an appropriate laser power and PMT gain to obtain the quenched donor image (Fig. 2e) and the sensitized acceptor/contaminated, uncorrected FRET image (uFRET) (Fig. 2f). The same cell was excited with acceptor excitation wavelength 514 nm with appropriate power and PMT gain to obtain the image Fig. 2g. The above mentioned PMT gain setting and the donor excitation power were used to collect the control images from the single expressed CFP (D) cells (Fig. 2a & b) to remove the donor spectral bleedthrough (DSBT) from uFRET. To remove the acceptor spectral bleedthrough (ASBT), images were collected using the YFP alone expressed cells with donor (Fig. 2c) and acceptor (Fig. 2d) excitation wavelengths. All these images were collected with appropriate filters [Dex 457 nm; Dem 485 nm; Aex 514 nm; Aem 535 nm][4].

There are various methods to assess the spectral bleed-through (SBT) contamination in the FRET image[4,28,34-41]. Our SBT correction approach works on the assumption that the double-labeled cells and single-labeled donor and acceptor cells, imaged under the same conditions, exhibit the same SBT dynamics[34,35]. The hurdle we had to overcome was the fact that we have three different cells (D, A, and D+A), where individual pixel locations cannot be compared. What can be compared, however, are pixels with matching fluorescence levels (Fig. 2: a/e & d/g). Our algorithm follows fluorescence levels pixel-by-pixel to establish the level of SBT in the single-labeled cells and then applies these values as a correction factor to the appropriate matching pixels of the double-labeled cell.

To establish PFRET (Processed FRET), i.e. the-contamination-removed FRET signal the following equation is applied[34,35]

$$PFRET = uFRET - DSBT - ASBT \quad \ldots(1)$$

where uFRET is contaminated FRET (signal in the FRET/acceptor channel); DSBT-donor spectral bleedthrough; ASBT-acceptor spectral bleedthrough.

Conventionally, energy transfer efficiency (E) is calculated by ratioing the donor image in the presence (I_{DA}) and absence (I_D) of acceptor. To execute this calculation, the acceptor in the double-label specimen

either has to be bleached or the donor fluorescence averages of two different cells (single and double label) with most likely different dynamics are used in the efficiency calculation. When using the algorithm as described, we indirectly obtain the I_D image by using the FRET image[34,35]. The sensitized emission in the acceptor channel is due to the quenching of the donor or energy transferred signal from the donor molecule in the presence of acceptor. Therefore, if we add the PFRET value back to the intensity of I_{DA}, pixel-by-pixel, we obtain I_D. Hence, the efficiency equation will be modified to obtain the new transfer efficiency (E_n) from the same cell which is shown in equation (3 or 4)

$$E = 1 - (I_{DA}/ I_D) \quad \ldots(2)$$

$$E_n = 1 - [I_{DA} / (I_{DA}+ PFRET)] \quad \ldots(3)$$

$$\text{or} \quad E_n = PFRET/(I_{DA}+ PFRET) \quad \ldots(4)$$

$$\text{where } I_D = I_{DA} + PFRET \quad \ldots(5)$$

The new efficiency (E_n) is calculated by generating a new I_D image by including the detector spectral sensitivity of donor and acceptor channel and the donor/acceptor quantum yields with FRET signal as shown in equation (6 or 7)[35].

$$E_n = 1 - \{I_{DA}/[I_{DA} + PFRET * (\psi_{dd}/\psi_{aa})*Q_d/Q_a]\} \quad \ldots(6)$$

Or the equation (6) can be rewritten as

$$En = PFRET*SS*QY/[(PFRET*SS*QY)+I_{DA}] \quad \ldots(7)$$

where

$$SS = (\psi_{dd}/\psi_{aa}) = [(\text{PMT gain of donor channel/PMT gain of acceptor channel})*(\text{spectral sensitivity of donor channel/spectral sensitivity of acceptor channel})] \quad \ldots(8)$$

$QY = Q_d/Q_a$ - Q_d and Q_a are donor and acceptor quantum yield, respectively

In equation (9) for estimating the distance between donor and acceptor, r, has changed to r_n. Förster's distance R_0 value was calculated for various fluorophore pairs[35]

$$r = R_0\{(1/E) - 1\}^{1/6} \quad \ldots(9)$$

$$r_n = R_0\{(1/E_n) - 1\}^{1/6} \quad \ldots(10)$$

Results and Discussion

Confocal and spectral imaging FRET microscopy are complimentary techniques, used here to characterize the intranuclear dimer formation for the

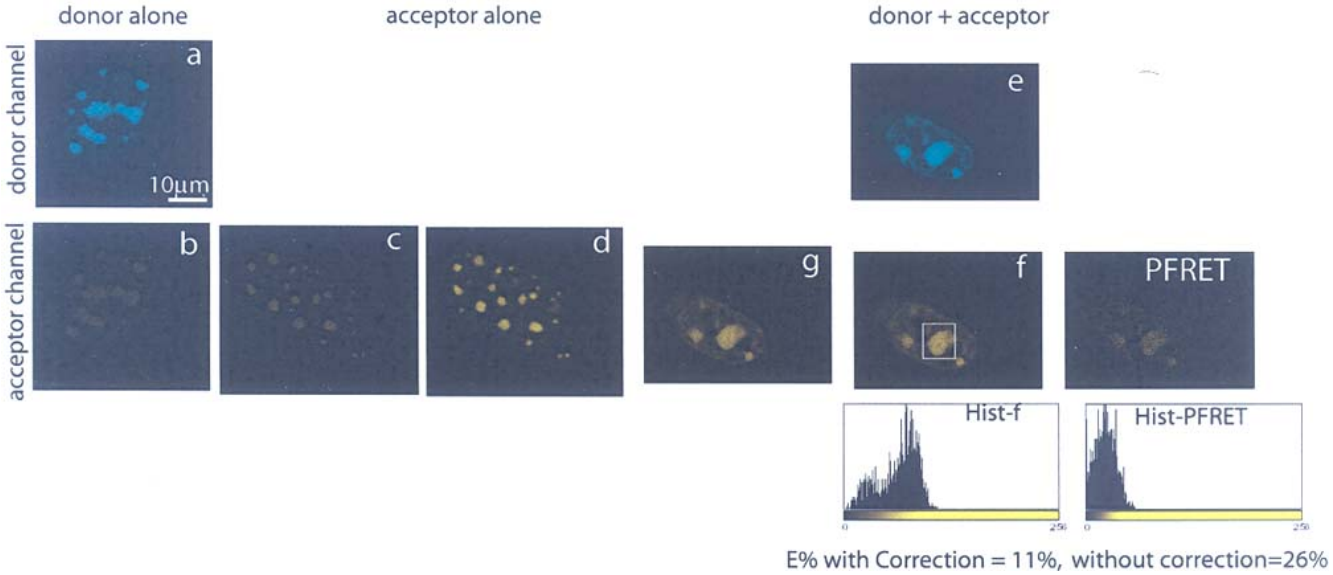

Fig. 2 — Dimerization of proteins in a living cell nucleus. Proteins were expressed with CFP- and YFP-C/EBPα in live mouse pituitary GHFT1-5 cell nucleus. Seven images (a-g) are required to remove the spectral contamination in the FRET image (f). The PFRET (processed FRET) image was obtained after removing the donor (DSBT) and acceptor (ASBT) spectral bleedthrough using the PFRET software[45]. The spectral bleedthrough varies depending on the excitation power for the donor and acceptor molecules. The respective histogram for the processed (Hist_PFRET) and the contaminated FRET (Hist_f) demonstrates the importance of removing the spectral bleedthrough signals. The energy transfer efficiency (E = 11%) was estimated after implementing the spectral bleedthrough correction and the detector spectral sensitivity correction for the donor and acceptor channel[35]. (See the text for more details)

transcription factor C/EBPα in living pituitary GHFT1-5 cells. Members of the C/EBP family of transcription factors are critical determinants of cell differentiation. C/EBPα controls the transcription of genes involved in energy, including those encoding anterior pituitary growth hormone (GH) and prolactin (PRL)[42]. C/EBPα is a basic region-leucine zipper (α-zip) transcription factor that forms dimers through contacts in the leucine zipper and binds to specific DNA elements via the basic region. Day *et al* have showed that GFP-tagged C/EBPα expressed in mouse pituitary GHFT1-5 cells was localized to subnuclear sites associated with pericentromeric heterochromatin[43], and this pattern was identical to that for the endogenous protein in differentiated mouse adipocytes[44]. Studies indicate that the b-zip region of C/EBPα (AA 244-358) fused to GFP was sufficient for subnuclear targeting of the fusion protein in pituitary GHFT1-5 cells[43]. Since this region contains the dimerization domain, we sought to determine whether the expressed fusion proteins were associated as dimers in these subnuclear sites.

To localize these protein dimerizations in the living cell nucleus, we used a laser scanning confocal FRET microscopy system. The cells, expressing Cyan (CFP) and Yellow fluorescent protein (YFP) were placed on the microscope stage. The images in Fig. 2a and Fig. 2b were acquired using CFP expressed (donor) cells using donor excitation wavelength (457 nm) in the donor and acceptor channels. The acceptor channel image represents the donor spectral bleedthrough (DSBT) image. In Fig. 2c the image was acquired using the donor excitation wavelength and the image in Fig. 2d was acquired using the acceptor alone expressed cells with the acceptor excitation wavelength. Fig. 2c represents the acceptor spectral bleedthrough (ASBT). Then, we used the double-label cells (donor and acceptor) and the images in Fig. 2e and Fig. 2f were collected. Fig. 2e represents the quenched donor image in the presence of acceptor. If the molecules are <10 nm apart, the donor molecule nonradiatively transfers energy to the acceptor molecule and sensitizes the acceptor/increases the signal (Fig. 2f) and consequently the donor image is quenched/decreased (Fig. 2e). Thus, the dimerized proteins were identified by the C-FRET methodology in the cell nucleus. The sensitized image (dimerized proteins), however, is contaminated with DSBT, ASBT and background noise. As explained in the FRET data analysis section[35], these images were processed to obtain the true FRET image (PFRET) from Fig. 2f. The image Fig. 2g was obtained as reference image from the doubly expressed cells to correct the ASBT.

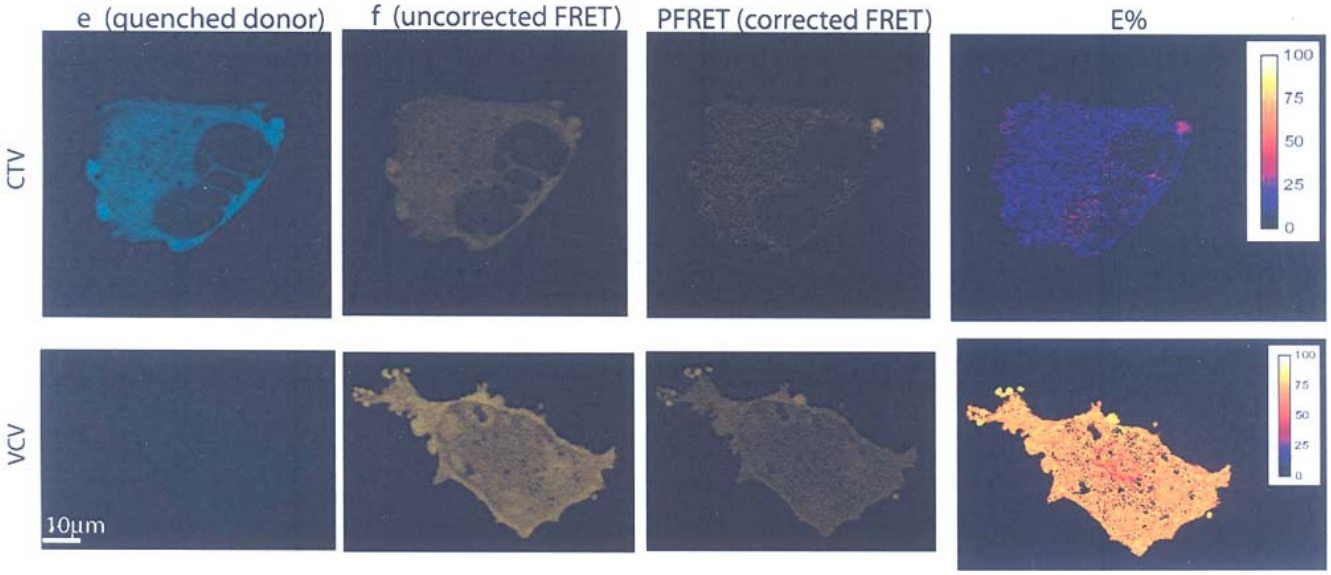

Fig. 3 — Demonstartion of occurrence of FRET using negative and positive controls. As described in the text and the literature[47], the CTV demonstrates that at 8 nm distance the PFRET signal is very weak and the energy transfer to donor to acceptor is very low, about 7%. On the other hand, in the case of VCV, the E% is about 70% and in this case there are two FRET de-excitation pathways instead of just one[47] as shown in CTV. In the case of higher E% the quenched donor image intensity is decreased considerably compared to the CTV quenched donor image. This clearly demonstrates that the C-FRET imaging system can monitor at low and high energy transfer signal.

As described, different cells are used to collect the DSBT and ASBT signal and it is impossible to directly subtract the bleedthrough from the image Fig. 1f by using the image in Fig. 2b and 2c. A simplistic method to remove the SBT is to take the mean intensity of the single labeled cells and subtract the same value from each pixel or establish a linear relationship (if it is linear) between intensity and SBT and subtract that; either way may work, but is likely to lead to over- or undercorrection[36, 41]. We prefer to use the pixel-by-pixel correction algorithm of the PFRET software[45] to obtain the PFRET image as shown in Fig. 2. The histogram clearly represents the contaminated signal from Fig. 1f versus the corrected PFRET image. Moreover, we estimated the energy transfer efficiency (E%) using equation (7) and showed that E% is higher (26%) before correction compared to after correction (11%). This convincingly shows that it is important for quantitative analysis to remove the spectral bleedthrough and other contamination from the FRET image with the most sensitive methodology available to avoid generating potentially spurious energy transfer efficiency data.

We have already demonstrated the occurrence of FRET with 15aa linker with CFP and YFP to show the occurrence of FRET[46]. There is no FRET signal observed if the proteins are colocalized or separated >10 nm[46]. As shown in Fig. 3, we have also conducted experiments with Cerulean and Venus fluorophores as a FRET pair standard[47]. The preparation and purification of these stoichiometry standards have been described to estimate the concentration of the donor and acceptor molecules[47]. In the CTV construct the Cerulean domain is separated from the Venus domain using a 229 amino-acid linker encoding the TRAF domain of human TRAF2[48]. The crystal structure of a TRAF domain has been solved, and predicts at least an 80 Å (8 nm) distance between Cerulean and Venus in the CTV construct[48]. In this situation the energy transfer efficiency is considerably reduced. As shown in Fig. 3 in the CTV panel, the E% value is in the range of 7%. On the other hand, with a Venus to Cerulean stoichiometry of 2:1, the Cerulean domain flanked on both sides with Venus domains provides a higher FRET efficiency than CTV because in its excited state Cerulean would have two FRET de-excitation pathways instead of just one[47]. As expected, the VCV provided higher efficiency about 70%. These images were acquired and processed using PFRET methodology as described in the Material and Methods section[35].

We have also implemented a spectral FRET (sFRET) technique to investigate protein dimerizations. As shown in Fig. 4, it is an effective technique to demonstrate the dimerization of proteins or any protein-protein interactions in living specimens by acquiring the respective spectra[7]. One needs to collect the control spectra of donor and acceptor as shown in Fig. 4I & 4II. These spectra will be used to unmix[29,30] or to remove the DSBT from the collected FRET spectra as shown in Fig. 4III. The Fig. 4III is

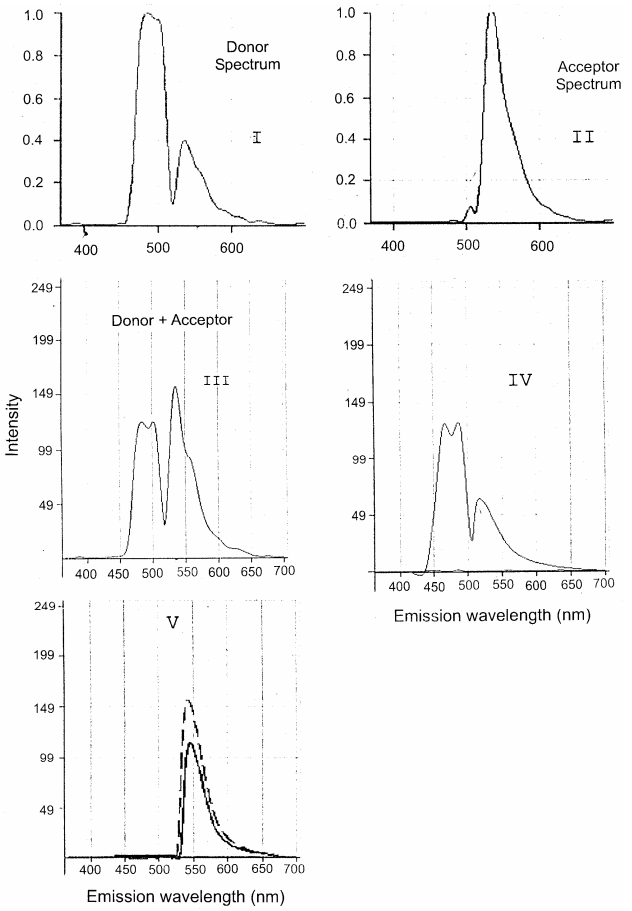

Fig. 4 — Spectral FRET imaging microscopy. Reference spectra (CFP, YFP) were established using cells expressing either CFP- or YFP-C/EBPα alone, and the emission spectra are shown in panel I and II. Images were then collected from cells expression both the CFP- and YFP-C/EBPα (Fig. 4III), and the signals were spectrally unmixed to reveal the donor bleed-through (IV) into the FRET channel (III), the corrected FRET signal is shown in Fig. 4V (broken line). The acceptor bleedthrough (ASBT, solid line) cannot be removed using spectral unmixing algorithm. We are in the process of developing an algorithm to separate the acceptor bleedthrough from the spectral FRET signal.

obtained by exciting the doubly-expressed cell with the donor excitation wavelength. The spectrum contains donor, acceptor and the FRET signal. The occurrence of FRET will indicate that in the acceptor emission wavelength (540 nm) region intensity peak is more than the donor (485 nm). By using the spectral unmixing algorithm[29-30] the donor bleed-through signal is separated as shown in Fig. 4IV which is similar to the donor-alone labeled cell (Fig. 4I). The FRET signal spectrum is shown in Fig. 4V (broken lines). Since the FRET spectrum falls in the same spectral area of the acceptor (see Fig. 4II) and the unmixing algorithm, however, cannot be used to remove the acceptor bleedthrough (solid line, Fig. 4V). We are in the process of developing an algorithm to separate the acceptor bleedthrough from the FRET signal.

It is also important to note that not all the labeled proteins participate in the energy transfer process as can be demonstrated in the lifetime FRET imaging methodology[17]. Proteins as FRET partners will interact only with those in the FRET proximity range (1-10 nm) and then usually with the closest and with the dipole-dipole coupling in an appropriate orientation (1-4). Therefore, there are non-FRET donors in most populations that nevertheless are included in the calculation of E%, which for this reason is called 'apparent' E%. On the other hand, using the FLIM-FRET techniques as demonstrated in the literature, it is possible to separate the FRET from the non-FRET donor lifetimes[12-19]. This technique is also independent of fluorophore concentrations and excitation intensity or wavelength and does not require SBT correction since one only follows the change in donor lifetime in the presence and the absence of acceptor[17-19,46]. For example, the lifetime of the donor (CFP) in the absence of the acceptor is 2.62 ns and in the presence of acceptor (CFP+YFP) the lifetime reduced at the particular pixel is about 1.9 ns, indicating the occurrence of FRET protein-protein interactions[46]. There is also a population of donor lifetimes close to that of the single donor specimen representing the non-FRET donors[12]. Even though the FLIM-FRET is complex and expensive, it is a sensitive technique to monitor the C/EBPα protein dimerization[4,12-13,17,46].

Conclusion

Light microscopy technology moved to the center stage in molecular imaging. There is no question that the described microscopy approaches in this paper will continue to assume greater and greater importance and develop into new directions, driven by advances in technological development and the growing number of cell biologist researchers who will routinely use this technology for protein imaging. Even though some of the microscopy techniques are somewhat more complex, they provide an unprecedented level of information about micromolecular interactions in cells under physiological conditions at very high temporal and spatial resolutions. New fluorophores such as various mutant form of green fluorescent proteins (GFPs) and in particular Quantum Dots will expand the usefulness of cellular imaging qualitatively and quantitatively and that will lead to more detailed insights in studying protein dynamics. C-FRET and Spectral Imaging techniques are commonly used for FRET imaging, but it is important to remember that the spectral bleedthrough needs to be removed to quantitate the FRET signal with confidence. On the other hand, while the FLIM-FRET technique is very challenging it provides very high temporal and spatial resolution and is able to monitor the dynamic process of the protein-protein interactions. Under the best of circumstances, different imaging approaches – sometimes near-simultaneously – for the same protein or cellular process of interest, will expand our ability to draw more accurate conclusions about the nature of cell function and structure.

Acknowledgment

The authors thank Ms Cindy Booker from Prof. Richard Day laboratory for preparing the cells and Mr Horst Wallrabe for providing valuable suggestions. We would like to thank the CTV and VCV constructs provided by Drs. Srinagesh Koushik and Steven Vogel, National Institute of Alcohol Abuse and Alcoholism (NIAAA), National Institutes of Health. The author acknowledges the funding support provided by the University of Virginia and the National Center for Research Resources (NCRR) a division of National Institutes of Health.

References

1 Hogg J, *The Microscope: History, Construction, and Application* (George Routledge and Sons, London), 1871.

2 Jones T, Memphis T N, *History of the Light Microscope*, <http://www.utmem.edu/personal/thjones/hist/c1.htm.>, 1997.

3 Periasamy A, *Methods in Cellular Imaging* (Oxford University Press, New York), 2001.

4 Periasamy A & Day R N, *Molecular Imaging:FRET Microscopy and Spectroscopy,* (Oxford University Press, New York), 2005.

5 Pawley J B, *Handbook of Biological Confocal Microscopy, 2nd edition*, (Plenum Press, New York), 1995.

6 Diaspro A, *Confocal and Two-photon Microscopy: Foundations, Applications, and Advances*. (John Wiley & Sons, New York), 2002.

7 Periasamy A, *Cellular imaging, in Encyclopedia of medical devices and instrumentation*, 2nd edition, edited by J G Webster (John-Wiley & Sons, New York) Vol. 2, 2006, 90.

8 Tsien R Y, Imagining imaging's future, *Nat Rev Mol Cell Biol*, 4 (2003) SS16.

9 Periasamy A & Day R N, Visualizing protein interactions in living cells using digitized GFP imaging and FRET microscopy, *Methods Cell Biol*, 58 (1999) 293.

10 Kraynov V S, Chamberlain C, Bokoch G M, Schwartz M A, Slabaugh S, & Hahn K M, Localized Rac activation dynamics visualized in living cells. *Science*, 290 (2000) 333.

11 Mills J D, Stone J R, Rubin D G, Melon D E, Okonkwo D O, Periasamy A, & Helm G A, Illuminating protein interactions in tissue using confocal and two-photon excitation fluorescent resonance energy transfer microscopy, *J Biomed Opt*, 8 (2003) 347.

12 Chen Y, & Periasamy A, Characterization of two-photon excitation fluorescence lifetime imaging microscopy for protein localization. *Microsc Res Tech*, 63 (2004) 72.

13 Sekar R B, & Periasamy A, Fluorescence resonance energy transfer (FRET) microscopy imaging of live cell protein localizations, *J Cell Biol*, 160 (2003) 629.

14 Redford G, & Clegg R B, Real-Time Fluorescence Lifetime Imaging and FRET using Fast Gated Image Intensifiers, in *Molecular Imaging: FRET Microscopy and Spectroscopy*, edited by Ammasi Periasamy & R N Day (Oxford University Press**,** New York) 2005, 193.

15 Krishnan R V, Masuda A, Centonze V E, & Herman B, Quantitative imaging of protein-protein interactions by multiphoton fluorescence lifetime imaging microscopy using a streak camera, *J Biomed Opt*, 8 (2003) 362.

16 Gerritsen H C, Asselbergs M A, Agronskaia A V, & Van Sark W G, Fluorescence lifetime imaging in scanning microscopes: acquisition speed, photon economy and lifetime resolution, *J Microsc*, 206 (2002) 218.

17 Elangovan M, Day R N, & Periasamy A, Nanosecond fluorescence resonance energy transfer-fluorescence lifetime imaging microscopy to localize the protein interactions in a single living cell, *J Microsc*, 205 (2002) 3.

18 Bastiaens P I, & Squire A, Fluorescence lifetime imaging microscopy: spatial resolution of biochemical processes in the cell, *Trends Cell Biol*, 9 (1999) 48.

19 Bacskai B J, Hickey G A, Skoch J, Kajdasz S T, Wang Y, Huang G F, Mathis C A, Klunk W E, & Hyman B T, Four-dimensional multiphoton imaging of brain entry, amyloid binding, and clearance of an amyloid-beta ligand in transgenic mice, *Proc Natl Acad Sci U S A* 100 (2003) 12462.

20 Clegg R M, Fluorescence resonance energy transfer, in *Fluorescence Imaging Spectroscopy and Microscopy*, edited by X F Wang & Brian Herman (John Wiley & Sons, New York) 137 1996, 179.

21 Förster T, Delocalized excitation and excitation transfer, *Modern Quantum Chemistry Part III: Action of Light and Organic Crystals*, edited by O Sinanoglu, (Academic Press, New York) 1965, 93.

22 Lakowicz J R, *Principles of Fluorescence Spectroscopy*, (Plenum Press, New York) 2nd ed., 1999.

23 Vogel S S, Thaler C, & Koushik S V, Fanciful FRET, Science STKE, 2006 (2006) re 2. (www.stke.org/)

24 Miyawaki A, Sawano A, & Kogure T, Lighting up cells: labeling proteins with fluorophores. *Nat Cell Biol*, Suppl (2003) S1.

25 Jares-Erijman E A, & Jovin T M, FRET imaging, *Nature BioTech*, 21 (2003) 1387.

26 Cubitt A B, Heim R, Adams S R, Boyd A E, Gross L A & Tsien R Y, Understanding, improving and using green fluorescent proteins, *Trends Biochem Sci*, 20 (1999) 448.

27 Lippincott-Schwartz J, Snapp E, *et al.* Studying protein dynamics in living cells. *Nature Rev Mol Cell Biol*, 2 (2001) 444.

28 Wallrabe H, & Periasamy A, FRET-FLIM microscopy and spectroscopy in the biomedical sciences, *Curr Opin Biotech*, 16 (2005) 19.

29 Dickinson M E, Simbuerger E, Zimmermann B, Waters C W, & Fraser S E, Multiphoton excitation spectra in biological samples, *J Biomed Opt*, 8 (2003) 329.

30 Dickinson M E, Bearman G, Tille S, Lansford R, & Fraser S E, Multi-spectral imaging and linear unmixing add a whole new dimension to laser scanning fluorescence microscopy, *Biotechniques*, 31 (2001) 1272.

31 Lew D, Brady H, Klausing K, Yaginuma K, Theill L E, Stauber C, Karin M, & Mellon P, GHF-1-promoter-targeted immortalization of a somatotropic progenitor cell results in dwarfism in transgenic mice, *Genes Dev*, 7 (1992) 683.

32 Lincoln A J, Williams S C, & Johnson P F, A revised sequence of the rat c/ebp gene, *Genes Dev*, 8 (1994) 1131.

33 Day R N, Visualization of Pit-1 transcription factor interactions in the living cell nucleus by fluorescence resonance energy transfer microscopy, *Mol Endo*, 12 (1998) 1410.

34 Elangovan M, Wallrabe H, Chen Y, Day R N, Barroso M, & Periasamy A, Characterization of one- and two-photon excitation resonance energy transfer microscopy, *Methods*, 29 (2003) 58.

35 Chen Y, Elangovan M, & Periasamy A, The algorithm-FRET data analysis, in *Molecular Imaging: FRET Microscopy and Spectroscopy*, edited by Ammasi Periasamy & R N Day (Oxford University Press, New York), 2005, 126.

36 Chen Y, & Periasamy A, Intensity range based quantitative FRET data analysis to localize the protein molecules in living cell nucleus, *J Fluorescence*, 16 (2006) 95.

37 Wallrabe H, Elangovan M, Burchard A, Periasamy A, & Barroso M, Confocal FRET microscopy to measure

clustering of receptor-ligand complexes in endocytic membranes. *Biophys J*, 85 (2003) 559.

38 Wallrabe H, Chen Y, Periasamy A, & Barroso M, Issues in confocal microscopy for quantitative FRET analysis, *Microsc Res Tech*, 69 (2006) 196.

39 Tron L, Szollosi J, Damjanovich S, Helliwell S, Arndt-Jovin D, & Jovin T, Flow cytometric measurement of fluorescence resonance energy transfer on cell surfaces. Quantitative evaluation of the transfer efficiency on a cell-by-cell basis, *Biophys J*, 45 (1984) 939.

40 Wouters F S, Bastiaens P I, Wirtz K W, & Jovin T M, FRET Microscopy demonstrates molecular association of non-specific lipid transfer protein (nsL-TP) with fatty acid oxidation enzymes in peroxisomes, *Embo J*, 17 (1998) 7179.

41 Gordon G W, Berry G, Liang X H, Levine B, & Herman B, Quantitative fluorescence resonance energy transfer measurements using fluorescence microscopy, *Biophy J*, 74 (1998) 2702.

42 Jacob K K, Stanley F M, CCAAT/enhancer-binding protein α is a physiological regulator of prolactin gene expression, *Endocrinology*, 140 (1999) 4542.

43 Day RN, Periasamy A, & Schaufele F, Fluorescence resonance energy transfer microscopy of localized protein interactions in the living cell nucleus, *Methods*, 25 (2001) 4.

44 Tang Q Q, & Lane M D, Activation and centromeric localization of CCAAT/enhancer-binding proteins during the mitotic clonal expansion of adipocyte differentiation, *Genes Dev*, 13 (1999) 2231.

45 Dedicated software is available for 8-bit FRET data analysis, www.circusoft.com. Software for 16-bit FRET data analysis written for ImageJ is available only for the FRET microscopy workshop participants. This workshop is organized annually during March. Visit the web site for details http://www.kcci.virginia.edu/workshop/index.php

46 Chen Y, Mills J D, & Periasamy A, Protein interactions in cells and tissues using FLIM and FRET, *Differentiation*. 71 (2003) 528.

47 Thaler C, Koushik S V, Blank P S, & Vogel S S, Quantitative multiphoton spectral imaging and its use for measuring resonance energy transfer, *Biophys J*, 89 (2005) 2736.